

# Caveolin-1 regulates oxidative stress-induced senescence in nucleus pulposus cells primarily via the p53/p21 signaling pathway *in vitro*

LEI DING<sup>1\*</sup>, QINGMIN ZENG<sup>1\*</sup>, JINGPING WU<sup>1</sup>, DEFANG LI<sup>1</sup>, HOULEI WANG<sup>1</sup>, WEI LU<sup>1</sup>, ZENGXIN JIANG<sup>1</sup> and GUOXIONG XU<sup>2</sup>

<sup>1</sup>Department of Orthopedic Surgery and <sup>2</sup>Central Laboratory, Jinshan Hospital, Fudan University, Shanghai 201508, P.R. China

Received February 12, 2017; Accepted September 12, 2017

DOI: 10.3892/mmr.2017.7789

**Abstract.** Previous studies have indicated that cellular senescence is a critical underlying mechanism of intervertebral disc degeneration. However, the precise mechanism by which cellular senescence accelerates disc degeneration has not been fully elucidated. Caveolin-1 has recently emerged as an important regulator of cellular senescence. Therefore, the aim of the present study was to investigate whether caveolin-1 is involved in nucleus pulposus (NP) cellular senescence during oxidative stress. PCR was used to detect caveolin-1 mRNA expression and protein expression was detected by western blotting. Caveolin-1 expression at the mRNA and protein levels was markedly increased following treatment with tert-butyl hydroperoxide, and an increase in premature senescence was observed, as determined by senescence-associated  $\beta$ -galactosidase staining and the decline of cellular proliferative ability. In addition, caveolin-1 gene expression was successfully knocked down by lentivirus-mediated RNA interference, which exerted a protective effect against the cellular senescence induced by oxidative stress. Notably, p53 and p21 protein expression, though not p16 protein expression, decreased with caveolin-1 silencing. The results suggested that caveolin-1 may be involved in NP cellular senescence during oxidative stress *in vitro*, mainly via the p53/p21 signaling pathway. Thus, caveolin-1 may represent a novel therapeutic target for the prevention of intervertebral disc degeneration.

## Introduction

Intervertebral disc (IVD) degeneration results in the pathogenesis of spinal disorders and is one of the main causes of lower back pain; it has also been associated with a high socioeconomic burden (1,2). The treatment and prevention of degenerative disc disease are restricted by a limited understanding of the mechanisms that regulate the processes underlying the development, maintenance and degeneration of the IVD (3). Previous studies have demonstrated in humans that the population of senescent cells is markedly increased in aged and degenerated discs *in vitro* and *in vivo* (4-6). Cellular senescence, characterized by irreversible growth arrest, is caused by a number of stressors, including reactive oxygen species and DNA damage, and decreases the cellular viability capacity for self-repair (7-9). In addition, senescent cells secrete multiple proinflammatory cytokines and matrix-degrading enzymes (5,10-13), that induce inflammation-associated stress and promote extracellular matrix degradation, which, in turn lead to the deterioration of the microenvironment and the promotion of the pathogenesis of degenerative diseases, such as IVD degeneration (5,10). Previous studies have also revealed that cellular senescence has a positive correlation with the progressive degree of IVD degeneration (14,15). These studies have indicated that cellular senescence may be a critical underlying mechanism of IVD degeneration. However, the precise mechanism by which cellular senescence accelerates disc degeneration has not been elucidated.

Caveolae are 50 to 100 nm flask-shaped invaginations of the plasma membrane (16). Caveolin-1 is a structural protein component of caveolae in the majority of cell types, and is thought to be involved in lipid transport, membrane trafficking and the regulation of a variety of signaling molecules (17,18). Caveolin-1 has also been associated with the premature senescent phenotype of several cell types, including human fibroblasts, articular chondrocytes and nucleus pulposus (NP) cells (11,19,20). Bartholomew *et al* (19) demonstrated that caveolin-1 is a novel MDM2 proto-oncogene binding protein and that it induced cellular senescence via the p53 signaling pathway. Volonte *et al* (11) also implicated caveolin-1 in cellular senescence via the inhibition of sirtuin 1 and the activation of the p53 signaling pathway in response to oxidative stress.

---

Correspondence to: Dr Jingping Wu, Department of Orthopedic Surgery, Jinshan Hospital, Fudan University, 1508 Longhang Road, Shanghai 201508, P.R. China  
E-mail: drwujp2015@163.com

\*Contributed equally

**Key words:** intervertebral disc degeneration, caveolin-1, senescence, nucleus pulposus, oxidative stress

In addition, caveolin-1 gene and protein expression have been detected in human IVD degeneration, and a role for caveolin-1 has been proposed in degenerative, as opposed to age-induced, alterations in the NP (4). A previous study reported that early IVD degeneration may be associated with the downregulation of canonical Wnt signaling and caveolin-1 expression, which, are thought to be essential to the physiology and preservation of notochordal cells (21). These observations demonstrated that the role of caveolin-1 in the development, maintenance and degeneration of IVD is still unclear. As cellular senescence may be involved in the mechanism of disc degeneration, elucidating the effects and the underlying mechanism of caveolin-1 in NP cellular senescence may provide promising strategies for the prevention of premature cellular senescence, and in turn, the prevention IVD degeneration.

The IVD is the largest avascular organ and in an oxidative microenvironment, the disposal of cellular waste in the IVD is hindered and cell viability is challenged (22-24). In the present study, oxidative stress was utilized to introduce cellular senescence in the rat NP in order to investigate the expression and mechanism of caveolin-1 in NP cells in response to this stress.

## Materials and methods

**Cell isolation and culture.** All animal experiments were approved by the Ethics Committee on Animal Experiments of Fudan University (Shanghai, China). A total of 2 male Sprague-Dawley rats (age, ~12 weeks; weight, 400 g) were used in the present study and were supplied by the Shanghai Public Health Center (Shanghai, China). Animals were housed with free access to food and water under a 12-h light/dark cycle, with a constant temperature (20-23°C) and humidity (55±5%). Rats were euthanized by cervical dislocation following anesthesia with pentobarbitalum natricum (1.5%) by intraperitoneal injection (50 mg/kg; Shanghai Shangxiao New Asia Pharmaceutical Co., Ltd., Shanghai, China; <http://www.xinyapharm.com>). Lumbar spines were obtained within 1 h of sacrifice, and the discs were carefully dissected under a microscope using aseptic conditions to obtain the NP. Tissues were sequentially treated with 0.25% trypsin (Sigma-Aldrich; Merck KGaA, Darmstadt, Germany) at 37°C for 2 h followed by 0.02% collagenase (Sigma-Aldrich; Merck KGaA) at 37°C for 24 h, then washed with phosphate-buffered saline (PBS). Subsequently, the cells were released from the matrix by centrifugation at 200 x g for 5 min at room temperature, seeded into 6-well plates (2x10<sup>4</sup> cells/well) and maintained in Dulbecco's modified Eagle's medium (DMEM; Gibco; Thermo Fisher Scientific, Inc., Waltham, MA, USA) supplemented with 10% fetal bovine serum (FBS; Gibco; Thermo Fisher Scientific, Inc.), 100 U/ml of penicillin (Beyotime Institute of Biotechnology, Nantong, China) and 100 µg/ml of streptomycin (Beyotime Institute of Biotechnology) under 5% CO<sub>2</sub> in a humidified incubator at 37°C. Primary cells were maintained in a high-density monolayer culture for 2 weeks. The cells were then trypsinized again and subcultured into 6-well plates; these cells were used in the subsequent experiments as secondary cells after reaching 80% confluence.

**Construction of lentivirus vectors.** A DNA template and oligonucleotides corresponding to the caveolin-1 gene (Gene ID:

NM\_001753; [www.ncbi.nlm.nih.gov/nuccore/NM\\_001753](http://www.ncbi.nlm.nih.gov/nuccore/NM_001753)) were targeted. The oligonucleotide sequences (Shanghai R&S Biotechnology Co., Ltd., Shanghai, China) were designed and synthesized as follows: Caveolin-1 small interfering (sh)RNA, forward, 5'-GACGUGGUCAAGAUUGACUTT-3' and reverse, 5'-AGUCAUUCUUGACCACGUCTT-3'. A control shRNA unassociated with these gene sequences was used as the negative control (NC): Caveolin-1 shRNA-NC, forward, 5'-CUGUGAUCCACUCUUUGAATT-3' and reverse, 5'-UUCAAA GAGUGGAUCACAGTT-3'. The combined sequences of the enhanced green fluorescent protein (GFP) gene and the caveolin-1 shRNA were cloned into the AseI and PmeI sites of the pLenti6.3-MCS vector (Shanghai R&S Biotechnology Co., Ltd., Shanghai, China) containing a cytomegalovirus-driven GFP reporter (25). All of the constructed plasmids (1 µg/µl; 5 µg) were confirmed by sequencing analysis, as previously described (26); prior to transfection into 293T cells (iCell Bioscience, Inc., Shanghai, China) using ViraPower lentiviral Packaging Mix (5 µg, Invitrogen; Thermo Fisher Scientific, Inc.) at 40% confluence (5x10<sup>5</sup> cells/well) in 10 cm plate. Supernatants containing lentiviruses were harvested at 96 h following transduction. Subsequent purification was performed using ultracentrifugation at 1610 x g and 4°C for 10 min. The isolated lentiviruses were stored at -80°C until use within 2 weeks; the lentivirus titre was 1.5x10<sup>6</sup>.

**Transfection of lentivirus.** Secondary cells were transferred to 6-well plates at a density of 5x10<sup>5</sup> cells/well in DMEM with 10% FBS without antibiotics the day prior to transduction procedures. Once cells had reached 80% confluency, cells were transfected with the aforementioned recombinant experimental or control lentivirus at a multiplicity of infection of 50 using polybrene (5 µg/ml; Sidansai Biotechnology Co., Ltd., Shanghai, China) for 24 h at 37°C. All cells were then refreshed with DMEM containing 10% FBS without antibiotics and cultured in DMEM with 10% FBS for 48 h. The transduction efficiency was determined by fluorescence microscopy, which was the average rate of green fluorescent cells in five fields (magnification, x100).

**Cell treatments.** To establish the cellular senescence model, secondary cells were treated with 70% tert-butyl hydroperoxide (t-BHP; Sigma-Aldrich; Merck KGaA) for 6 h at 37°C, and the sublethal final concentration was observed to be 100 µmol/l. Cells treated with t-BHP were infected with either the caveolin-1 short hairpin (sh)RNA vector or the NC vector, which, were termed NP-LV and NP-LV-NC, respectively. An additional untransfected group treated with t-BHP was used as the control group, which, was termed NP-CTR. Untransfected cells treated under normal conditions without t-BHP treatment formed the normal control group, termed NP-NOM. All four treatment groups were incubated under DMEM with 10% FBS for 72 h at 37°C; the subsequent experiments were performed using cells at different time points throughout this 72 h period.

**Senescence-associated β-galactosidase (SA-β-gal) staining.** SA-β-gal staining was performed using a SA-β-gal staining kit (Cell Signaling Technology, Inc., Danvers, MA, USA) according to the manufacturer's instructions. Briefly, cells were washed twice with PBS and fixed with 3% formaldehyde

for 15 min at 37°C. Cells were then incubated overnight at 37°C with the kit staining solution. Cells were photographed under reflected light using a digital high-fidelity fluorescence microscope (VH-8000; Keyence Corporation, Osaka, Japan). A total of 5 fields, that were distributed throughout the well, were counted (magnification, x200), and the average rate of positive staining was recorded.

**Measurement of proliferation.** The proliferation of NP cells exposed to t-BHP treatment was assessed by cell counting kit-8 (CCK-8; Beyotime Institute of Biotechnology) at 0, 24, 48 and 72 h. Briefly, cells were replated at  $1 \times 10^4$  cells/well in a 96-well plate, and were then incubated with 10  $\mu$ l CCK-8 solution at 37°C for 2 h. The mixtures were analyzed with an Epoch Multi-Volume Spectrophotometer System (BioTek Instruments, Inc., Winooski, VT, USA) at an absorbance of 490 nm. Proliferative activities were each calculated as the change in absorbance at 490 nm.

**Reverse transcription-quantitative polymerase chain reaction (RT-qPCR).** RT-qPCR was performed to detect caveolin-1 mRNA in the different treatment groups at 24, 36 and 72 h; GAPDH was used as an internal standard control. Briefly, total RNA was extracted using TRIzol reagent (Invitrogen; Thermo Fisher Scientific, Inc.) following the manufacturer's instructions. Single-strand cDNA templates were prepared from 1  $\mu$ g total RNA using the RT-for-PCR kit (Clontech Laboratories, Inc., Mountainview, CA, USA). Specific cDNAs were then amplified by PCR using the following primers: Caveolin-1, forward, 5'-AAGGAGATCGACCTG-3' and reverse, 5'-GGA ATAGACACGGCTG-3'; GAPDH, forward, 5'-CCCAATGT ATCCGTTGTG-3' and reverse, 5'-CTCAGTGTAGCCAG GATGC-3'. PCR amplification from cDNA was performed using the Takara TP800 Thermal Cycler Dice (Takara Bio, Inc., Otsu, Japan) with a final volume of 20  $\mu$ l [2X SYBR Green Mix 10  $\mu$ l (Invitrogen; Thermo Fisher Scientific, Inc.), 1  $\mu$ l primer mix, 1  $\mu$ l template DNA and 8  $\mu$ l diethylpyrocarbonate water]. The thermocycling conditions were as follows: Initial denaturation at 95°C for 2 min, followed by 40 cycles of denaturation at 95°C for 15 sec, annealing at 59°C for 20 sec and elongation at 72°C for 20 sec, and then a final extension at 72°C for 10 min. PCR products were subjected to amplification curve analysis and quantified using SYBR Green (Invitrogen; Thermo Fisher Scientific, Inc.). The data were normalized to GAPDH and quantified using the  $2^{-\Delta\Delta Cq}$  method (27,28).

**Western blot analysis.** The protein expression levels of caveolin-1, p53, p21 and p16 were detected by western blot analysis following 72 h of cell treatment. Total protein was extracted with SDS-PAGE Sample Loading Buffer 5X (cat. no. P0015, Beyotime Institute of Biotechnology). The total protein concentration was determined by a bicinchoninic acid assay (Sigma-Aldrich; Merck KGaA). Protein (20  $\mu$ g/lane) extracts were separated by 8-12% SDS-PAGE and were then transferred to polyvinylidene difluoride membranes (EMD Millipore, Billerica, MA, USA). The membranes were blocked with 5% non-fat dry milk in Tris-buffered saline with 0.1% Tween (TBST) for 1 h at 37°C, and incubated overnight at 4°C in TBST with the following primary antibodies: Mouse monoclonal anti-caveolin-1 (dilution 1:1,000; cat.

no. AF0087; Beyotime Institute of Biotechnology), mouse monoclonal anti-p53 (dilution 1:1,000; cat. no. AF0255; Beyotime Institute of Biotechnology), mouse monoclonal anti-p21 (dilution 1:500; cat. no. AP021; Beyotime Institute of Biotechnology), polyclonal rabbit anti-p16 (dilution 1:1,000; cat. no. SAB4500072; Sigma-Aldrich; Merck KGaA) and mouse monoclonal anti- $\beta$ -actin (dilution 1:2,000; cat. no. AF0003; Beyotime Institute of Biotechnology). The membranes were then further incubated with a horseradish peroxidase-conjugated goat anti-rabbit IgG secondary antibody (dilution 1:5,000; cat. no. A0208; Beyotime Institute of Biotechnology) for 1 h at room temperature, prior to treatment with Electrochemiluminescence Plus (Tanon Science and Technology Co., Ltd., Shanghai, China), according to the manufacturer's protocol.

**Statistical analysis.** All measurements were carried out using the same instrument under the same experimental conditions and were independently performed at least three times to ensure consistency. Statistical analyses were performed using SPSS 16.0 software (SPSS, Inc., Chicago, IL, USA). Data are expressed as the mean  $\pm$  standard deviation. Significant differences were analyzed with a one-way analysis of variance. Bonferroni was used for multiple comparisons.  $P < 0.05$  was considered to indicate a statistically significant difference.

## Results

**Effect of oxidative stress on NP cells.** To evaluate the effects of t-BHP-induced oxidative stress on NP cells, the percentage of SA- $\beta$ -gal-positive cells and the cellular proliferative rate were assessed. Premature senescence of NP cells was investigated following treatment with t-BHP and culture for 72 h. As is shown in Fig. 1A, the percentage of SA- $\beta$ -gal-positive cells was significantly higher in the NP-CTR group when compared with the NP-NOM group at 72 h ( $34.25 \pm 1.45\%$  vs.  $5.60 \pm 0.68\%$ ;  $P < 0.05$ ). In addition, the proliferative rate of NP-CTR cells gradually decreased with increasing time when compared with NP-NOM cells, and at 72 h the proliferative activity decreased to nearly half that of the NP-NOM control group ( $0.82 \pm 0.15\%$  vs.  $1.60 \pm 0.21\%$ ;  $P < 0.05$ ; Fig. 1B). Notably, caveolin-1 expression at the mRNA and protein level was markedly increased following treatment with t-BHP which, is in agreement with the increase observed in the percentage of SA- $\beta$ -gal-positive cells and the reduction in cellular proliferative ability (Fig. 1C-E).

**Silencing caveolin-1 expression by lentiviral-mediated RNA interference.** Lentiviral shRNA was successfully constructed and confirmed by sequencing analysis; the transduction rate of the lentivirus was  $\sim 90\%$  at 48 h (Fig. 2A). Caveolin-1 expression was assessed by RT-qPCR and western blot analysis following treatment with t-BHP. As shown in Fig. 2B, the mRNA levels of caveolin-1 decreased in the NP-LV group at 24, 36 and 48 h when compared with the NP-CTR group; however, no marked difference was detected when comparing the NP-CTR and NP-LV-NC groups. Similarly, the caveolin-1 protein level also decreased in the NP-LV group at 72 h and was markedly decreased when compared with the NP-CTR group (Fig. 2C). These results demonstrated that caveolin-1 gene expression

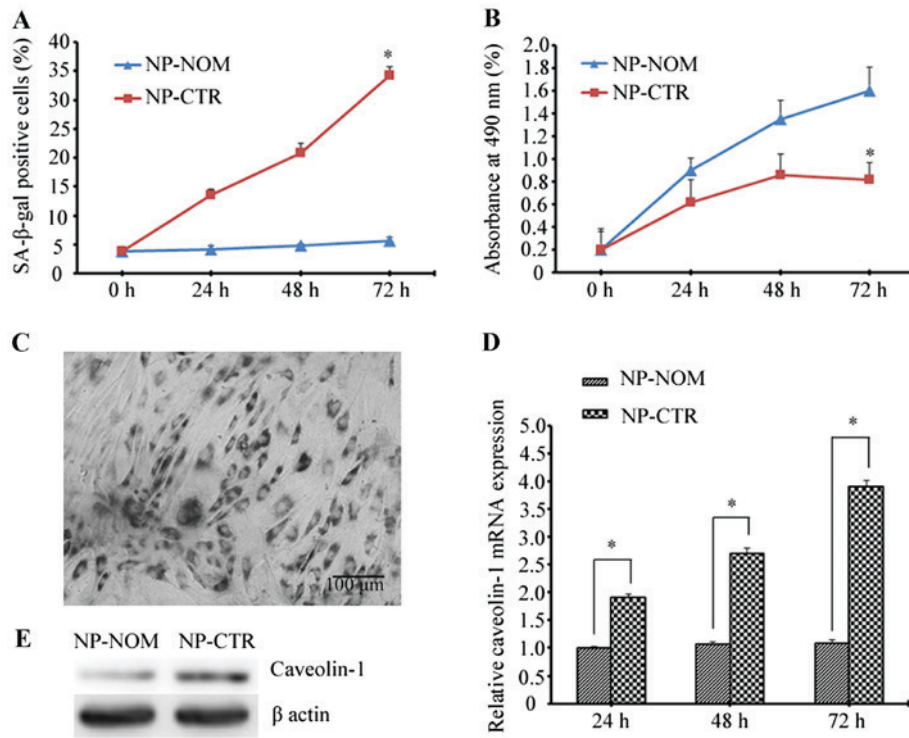


Figure 1. Evaluation of the effects of t-BHP-induced oxidative stress on NP cells. (A) The percentage of senescent cells induced by oxidative stress was determined by SA-β-gal positive staining. (B) Cellular proliferative abilities were assessed in cells with or without the induction of oxidative stress. \*P<0.05 vs. NP-NOM. (C) A representative image of SA-β-gal positive NP cells (magnification, x200; scale bar, 100 μm). (D) Quantitative analysis of caveolin-1 mRNA expression assessed by reverse transcription-quantitative polymerase chain reaction at 24, 48 and 72 h following t-BHP-induced oxidative stress. \*P<0.05, as indicated. (E) Representative western blotting image showing caveolin-1 expression in cells with or without t-BHP-induced oxidative stress. t-BHP, tert-butyl hydroperoxide; NP, nucleus pulposus; SA-β-gal, senescence-associated β-galactosidase; NP-NOM group, cells cultured under normal conditions without t-BHP treatment; NP-CTR group, control cells treated with t-BHP only.

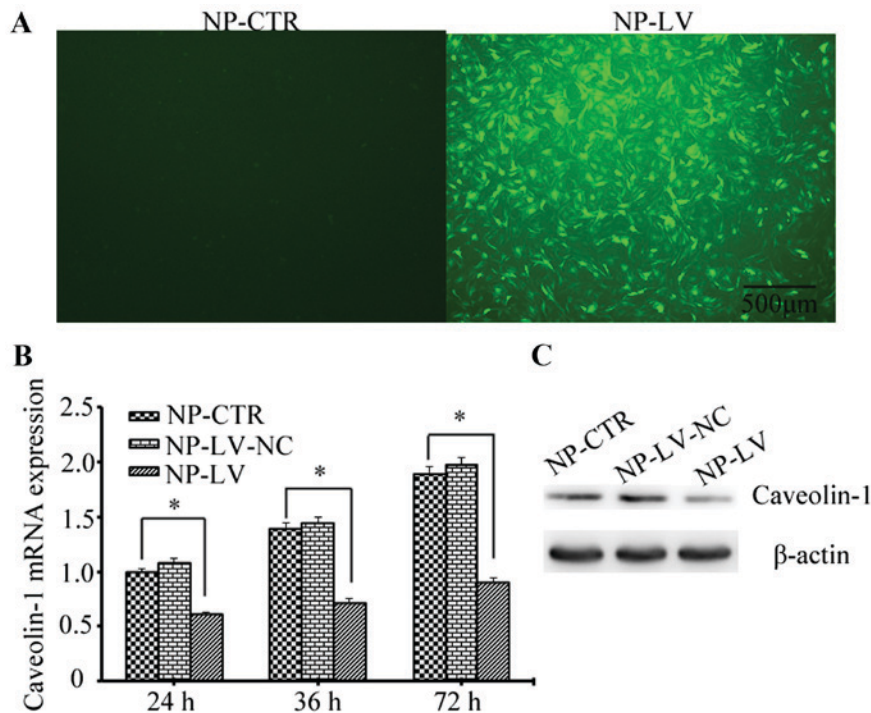


Figure 2. Evaluation of the caveolin-1 silencing mediated by lentiviral short hairpin RNA. (A) The transduction efficiency was ~90%, as determined by fluorescence microscopy (magnification, x40; scale bars, 500 μm). (B) Assessment of caveolin-1 mRNA expression by reverse transcription-quantitative polymerase chain reaction at 24, 48 and 72 h following t-BHP-induced oxidative stress. In the NP-LV group caveolin-1 mRNA levels were reduced to ~46% of those produced by the NP-CTR group at 72 h. \*P<0.05, as indicated. (C) Protein levels were assessed by western blotting. The expression of caveolin-1 was markedly decreased in the NP-LV group at 72 h when compared with the other two groups. t-BHP, tert-butyl hydroperoxide; NP, nucleus pulposus; NP-CTR group, control cells treated with t-BHP only; NP-LV group, cells treated with t-BHP and lentivirus; NP-LV-NC, cells treated with t-BHP and negative control lentivirus.

was successfully knocked down by lentivirus-mediated RNA interference.

**Caveolin-1-mediated premature senescence induced by oxidative stress.** To determine whether caveolin-1 mediated oxidative stress-induced cellular senescence, the present study quantitatively assessed the percentage of SA- $\beta$ -gal-positive cells and the proliferative rate following silencing of caveolin-1 expression. As shown in Fig. 3, when caveolin-1 was knocked down in the NP-LV group, the increase in SA- $\beta$ -gal-positive cells at 72 h was not as marked when compared with the NP-CTR group ( $20.56\pm 1.28\%$  vs.  $34.25\pm 1.45\%$ ;  $P<0.05$ ; Fig. 3A). At 72 h, more proliferative cells were observed in the NP-LV group than in the NP-CTR group when caveolin-1 expression decreased ( $1.22\pm 0.20\%$  vs.  $0.82\pm 0.15\%$ ;  $P<0.05$ ; Fig. 3B).

**Caveolin-1 induced senescence via the p53/p21 signaling pathway under oxidative stress.** Cellular senescence primarily occurs via two signaling pathways: The p16 pathway and the p53/p21 pathway (16). In the present study, the expression of the p53 protein increased under oxidative stress in the NP-CTR and NP-LV-NC groups when compared with NP-NOM (Fig. 4). The levels of the p21 protein, a pro-senescence modulator of p53 activity, were also increased under t-BHP-induced oxidative stress in the two groups (29). In addition, inhibition of caveolin-1 expression markedly decreased p53 and p21 protein expression levels in the NP-LV group. Notably, the decrease in p53 and p21 protein expression were associated with the decrease in SA- $\beta$ -gal-positive cells and the recovery of cellular proliferative ability. By contrast, there was no marked difference in p16 protein levels among the three groups when compared with NP-NOM.

## Discussion

A previous study has reported that cellular senescence is widespread in degenerated IVD and is positively associated with degenerative grade (15). In addition, higher levels of cell senescence have been observed in degenerated discs than in age-matched non-degenerated discs (30,31). Senescence results in the deterioration of the microenvironment due to the secretion of inflammatory cytokines and catabolic enzymes, which, in turn accelerate IVD degeneration (10). The IVD microenvironment is unique and is characterized by a limited nutrient supply, hypoxia (32), hypertonicity, increased acidity, varied mechanical loading, and continuous and unavoidable exposure to reactive oxygen species (ROS) (24). However, whether excessive oxidative stress is the main result of premature senescence in the NP remains unclear. In addition, the potential mechanism underlying senescence in the NP also requires elucidation. Therefore, the aim of the present study was to investigate the associations and mechanisms underlying oxidative stress-associated senescence in NP cells.

There are two types of cellular senescence: Replicative senescence (RS) and stress-induced premature senescence (SIPS) (31). RS is dependent on the gradual shortening of telomeres at the ends of chromosomes (29). By contrast, certain extrinsic stresses, such as ultraviolet irradiation (33) and oxidative stress (34,35), trigger the type of premature

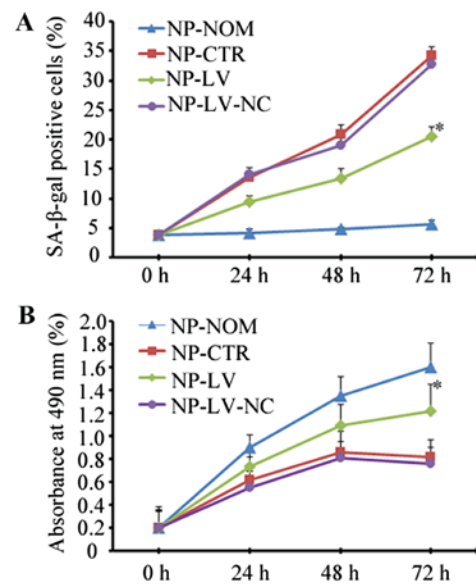


Figure 3. Caveolin-1 mediated oxidative stress-induced cellular senescence. (A) Caveolin-1 silencing induced a decrease in senescent cells when compared with NP-CTR, as determined by SA- $\beta$ -gal staining. (B) Caveolin-1 silencing was associated with the recovery of proliferative ability. \* $P<0.05$  vs. NP-CTR. SA- $\beta$ -gal, senescence-associated  $\beta$ -galactosidase; NP, nucleus pulposus; t-BHP, tert-butyl hydroperoxide; NP-NOM group, cells cultured under normal conditions without t-BHP treatment; NP-CTR group, control cells treated with t-BHP only; NP-LV group, cells treated with t-BHP and lentivirus; NP-LV-NC, cells treated with t-BHP and negative control lentivirus.

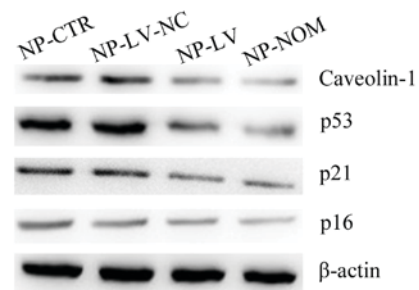


Figure 4. Evaluation of the expression of proteins associated with senescence pathways, as shown by western blotting. Silencing of caveolin-1 expression decreased p53 and p21 protein levels in the NP-LV group when compared with the NP-CTR and NP-LV-NC groups. However, no marked difference in p16 protein levels was observed among the three groups. NP, nucleus pulposus; t-BHP, tert-butyl hydroperoxide; NP-NOM group, cells cultured under normal conditions without t-BHP treatment; NP-CTR group, control cells treated with t-BHP only; NP-LV group, cells treated with t-BHP and lentivirus; NP-LV-NC, cells treated with t-BHP and negative control lentivirus.

senescence termed SIPS. In the present study, the percentage of SA- $\beta$ -gal-positive cells increased following treatment with t-BHP, and inhibition of cellular proliferation was also observed. This result indicated that more cellular senescence was triggered by oxidative stress in NP cells; this was consistent with previous findings (22). These results suggested that the induction of cellular SIPS by excess ROS may be the reason for the accelerated degeneration of discs.

In addition, the mRNA and protein levels of caveolin-1 were markedly increased following treatment with t-BHP, indicating that caveolin-1 may be involved in the process of cellular

premature senescence. A previous report demonstrated that caveolin-1 serves a major role in RS and SIPS (16). A recent study revealed that caveolin-1 increased mouse embryonic fibroblast senescence by inhibiting sirtuin 1 (11). The importance of caveolin-1 in RS was supported by a previous study that demonstrated that senescent bone marrow stromal cells expressed higher levels of caveolin-1 than younger cells (36). In addition, mouse embryonic fibroblasts prematurely induced by oxidative stress were inhibited in caveolin-1 null mice (19). In the present study, the results indicated that caveolin-1 expression and cellular senescence may be associated in NP cells. Caveolin-1 was successfully silenced by lentiviral shRNA-mediated RNA interference, and mRNA and protein expression decreased following the transfection of the NP-LV cells. In addition, cellular senescence induced by oxidative stress was decreased in the NP-LV group, as demonstrated by the decrease in the percentage of SA- $\beta$ -gal-positive cells and the recovery of proliferative ability. These results indicated that caveolin-1 may be involved in the increased premature senescence of NP cells induced by oxidative stress *in vitro*. Silencing of caveolin-1 protected cells against premature senescence and increased cellular proliferative ability.

Cellular senescence primarily occurs via two pathways: The p16 pathway and the p53/p21<sup>cip</sup> pathway (16). In the present study, the potential pathway associated with caveolin-1 and oxidative stress-induced senescence in NP cells was evaluated. Previous studies have revealed that caveolin-1 may be involved in the two pathways in SIPS in different cells (11,16,37). Human cells from the degenerated NP have provided evidence of cellular senescence and express high levels of caveolin-1; they have also revealed a positive association with the SIPS biomarker 16INK4a (4). Volonte *et al* (11) demonstrated that overexpression of caveolin-1 generated stress-induced premature senescence in the p53 wild-type, though not the p53 knockout, mouse embryonic fibroblasts. Notably, in the present study caveolin-1 was positively associated with p53 and p21, and silencing caveolin-1 resulted in the reduction of p53 and p21 expression in the NP-LV group. By contrast, no marked decrease in p16 expression was observed in the NP-LV group. These results indicated that caveolin-1 may be primarily involved in NP cell senescence via the p53/p21 signaling pathway under oxidative stress *in vitro*; however, these results differ to those reported by Heathfield *et al* (4). Pathogenesis of IVD degeneration is a chronic process *in vivo* and the two different pathways can overlap, thus, p16 expression may also be associated with chronic SIPS and RS (16). In the present study, the use of transient oxidative stress may have produced different results.

In conclusion, the results of the present study provide potential strategies for the prevention premature NP cellular senescence. However, additional experiments involving the overexpression of caveolin-1 were not conducted and future research including *in vivo* experiments are required in order to determine whether the silencing of the caveolin-1 expression is able to delay the degeneration of the IVD.

### Acknowledgements

The present study was supported by the Shanghai Municipality Health Bureau (grant nos. 201640101 and 2014-399) and

the Jinshan Science and Technology Committee (grant no. 2016-3-06).

### References

- Hoy D, Brooks P, Woolf A, Blyth F, March L, Bain C, Baker P, Smith E and Buchbinder R: Assessing risk of bias in prevalence studies: Modification of an existing tool and evidence of interrater agreement. *J Clin Epidemiol* 65: 934-939, 2012.
- de Schepper EI, Damen J, van Meurs JB, Ginai AZ, Popham M, Hofman A, Koes BW and Bierma-Zeinstra SM: The association between lumbar disc degeneration and low back pain: The influence of age, gender, and individual radiographic features. *Spine (Phila Pa 1976)* 35: 531-536, 2010.
- Raj PP: Intervertebral disc: Anatomy-physiology-pathophysiology-treatment. *Pain Pract* 8: 18-44, 2008.
- Heathfield SK, Le Maitre CL and Hoyland JA: Caveolin-1 expression and stress-induced premature senescence in human intervertebral disc degeneration. *Arthritis Res Ther* 10: R87, 2008.
- Wang F, Cai F, Shi R, Wang XH and Wu XT: Aging and age related stresses: A senescence mechanism of intervertebral disc degeneration. *Osteoarthritis Cartilage* 24: 398-408, 2016.
- Le Maitre CL, Freemont AJ and Hoyland JA: Accelerated cellular senescence in degenerate intervertebral discs: A possible role in the pathogenesis of intervertebral disc degeneration. *Arthritis Res Ther* 9: R45, 2007.
- van Deursen JM: The role of senescent cells in ageing. *Nature* 509: 439-446, 2014.
- Muñoz-Espín D and Serrano M: Cellular senescence: From physiology to pathology. *Nat Rev Mol Cell Biol* 15: 482-496, 2014.
- Sharpless NE and Sherr CJ: Forging a signature of *in vivo* senescence. *Nat Rev Cancer* 15: 397-408, 2015.
- Dimozi A, Mavrogonatou E, Sklirou A and Kletsas D: Oxidative stress inhibits the proliferation, induces premature senescence and promotes a catabolic phenotype in human nucleus pulposus intervertebral disc cells. *Eur Cell Mater* 30: 89-102, 2015.
- Volonte D, Zou H, Bartholomew JN, Liu Z, Morel PA and Galbiati F: Oxidative stress-induced inhibition of Sirt1 by caveolin-1 promotes p53-dependent premature senescence and stimulates the secretion of interleukin 6 (IL-6). *J Biol Chem* 290: 4202-4214, 2015.
- Kletsas D: Senescent cells in the intervertebral disc: Numbers and mechanisms. *Spine J* 9: 677-678, 2009.
- Acosta JC, Banito A, Wuestefeld T, Georgilis A, Janich P, Morton JP, Athineos D, Kang TW, Lasitschka F, Andrusis M, *et al*: A complex secretory program orchestrated by the inflammasome controls paracrine senescence. *Nat Cell Biol* 15: 978-990, 2013.
- Kim KW, Chung HN, Ha KY, Lee JS and Kim YY: Senescence mechanisms of nucleus pulposus chondrocytes in human intervertebral discs. *Spine J* 9: 658-666, 2009.
- Gruber HE, Ingram JA, Davis DE and Hanley EN Jr: Increased cell senescence is associated with decreased cell proliferation *in vivo* in the degenerating human annulus. *Spine J* 9: 210-215, 2009.
- Zou H, Stoppani E, Volonte D and Galbiati F: Caveolin-1, cellular senescence and age-related diseases. *Mech Ageing Dev* 132: 533-542, 2011.
- Parton RG and Simons K: The multiple faces of caveolae. *Nat Rev Mol Cell Biol* 8: 185-194, 2007.
- Smart EJ, Graf GA, McNiven MA, Sessa WC, Engelman JA, Scherer PE, Okamoto T and Lisanti MP: Caveolins, liquid-ordered domains, and signal transduction. *Mol Cell Biol* 19: 7289-7304, 1999.
- Bartholomew JN, Volonte D and Galbiati F: Caveolin-1 regulates the antagonistic pleiotropic properties of cellular senescence through a novel Mdm2/p53-mediated pathway. *Cancer Res* 69: 2878-2886, 2009.
- Dai SM, Shan ZZ, Nakamura H, Masuko-Hongo K, Kato T, Nishioka K and Yudoh K: Catabolic stress induces features of chondrocyte senescence through overexpression of caveolin 1: Possible involvement of caveolin 1-induced down-regulation of articular chondrocytes in the pathogenesis of osteoarthritis. *Arthritis Rheum* 54: 818-831, 2006.

21. Smolders LA, Meij BP, Onis D, Riemers FM, Bergknut N, Wubbolts R, Grinwis GC, Houweling M, Groot Koerkamp MJ, van Leenen D, *et al*: Gene expression profiling of early intervertebral disc degeneration reveals a down-regulation of canonical Wnt signaling and caveolin-1 expression: Implications for development of regenerative strategies. *Arthritis Res Ther* 15: R23, 2013.
22. Hou G, Lu H, Chen M, Yao H and Zhao H: Oxidative stress participates in age-related changes in rat lumbar intervertebral discs. *Arch Gerontol Geriatr* 59: 665-669, 2014.
23. Nasto LA, Robinson AR, Ngo K, Clauson CL, Dong Q, St Croix C, Sowa G, Pola E, Robbins PD, Kang J, *et al*: Mitochondrial-derived reactive oxygen species (ROS) play a causal role in aging-related intervertebral disc degeneration. *J Orthop Res* 31: 1150-1157, 2013.
24. Zhang F, Zhao X, Shen H and Zhang C: Molecular mechanisms of cell death in intervertebral disc degeneration (review). *Int J Mol Med* 37: 1439-1448, 2016.
25. Ding L, Wu JP, Xu G, Zhu B, Zeng QM, Li DF and Lu W: Lentiviral-mediated RNAi targeting caspase-3 inhibits apoptosis induced by serum deprivation in rat endplate chondrocytes in vitro. *Braz J Med Biol Res* 47: 445-451, 2014.
26. Sanger F and Coulson AR: A rapid method for determining sequences in DNA by primed synthesis with DNA polymerase. *J Mol Biol* 94: 441-448, 1975.
27. Ding L, Wu J, Li D, Wang H, Zhu B, Lu W and Xu G: Effects of CCN3 on rat cartilage endplate chondrocytes cultured under serum deprivation in vitro. *Mol Med Rep* 13: 2017-2022, 2016.
28. Livak KJ and Schmittgen TD: Analysis of relative gene expression data using real-time quantitative PCR and the 2(-Delta Delta C(T)) method. *Methods* 25: 402-408, 2001.
29. Ben-Porath I and Weinberg RA: The signals and pathways activating cellular senescence. *Int J Biochem Cell Biol* 37: 961-976, 2005.
30. Jeong SW, Lee JS and Kim KW: In vitro lifespan and senescence mechanisms of human nucleus pulposus chondrocytes. *Spine J* 14: 499-504, 2014.
31. Feng C, Liu H, Yang M, Zhang Y, Huang B and Zhou Y: Disc cell senescence in intervertebral disc degeneration: Causes and molecular pathways. *Cell Cycle* 15: 1674-1684, 2016.
32. Chen JW, Li B, Yang YH, Jiang SD and Jiang LS: Significance of hypoxia in the physiological function of intervertebral disc cells. *Crit Rev Eukaryot Gene Expr* 24: 193-204, 2014.
33. Zhou BR, Guo XF, Zhang JA, Xu Y, Li W, Wu D, Yin ZQ, Permatasari F and Luo D: Elevated miR-34c-5p mediates dermal fibroblast senescence by ultraviolet irradiation. *Int J Biol Sci* 9: 743-752, 2013.
34. Shin JH, Jeon HJ, Park J and Chang MS: Epigallocatechin-3-gallate prevents oxidative stress-induced cellular senescence in human mesenchymal stem cells via Nrf2. *Int J Mol Med* 38: 1075-1082, 2016.
35. Kiyoshima T, Enoki N, Kobayashi I, Sakai T, Nagata K, Wada H, Fujiwara H, Ookuma Y and Sakai H: Oxidative stress caused by a low concentration of hydrogen peroxide induces senescence-like changes in mouse gingival fibroblasts. *Int J Mol Med* 30: 1007-1012, 2012.
36. Sun C, Wang N, Huang J, Xin J, Peng F, Ren Y, Zhang S and Miao J: Inhibition of phosphatidylcholine-specific phospholipase C prevents bone marrow stromal cell senescence in vitro. *J Cell Biochem* 108: 519-528, 2009.
37. Kortum RL, Fernandez MR, Costanzo-Garvey DL, Johnson HJ, Fisher KW, Volle DJ and Lewis RE: Caveolin-1 is required for kinase suppressor of Ras 1 (KSR1)-mediated extracellular signal-regulated kinase 1/2 activation, H-RasV12-induced senescence, and transformation. *Mol Cell Biol* 34: 3461-3472, 2014.